EPSC Abstracts
Vol. 10, EPSC2015-69, 2015
European Planetary Science Congress 2015

Planets and satellites: tectonic twins

Kochemasov G.G. IGEM of the Russian Academy of Sciences, 119017 Moscow, kochem.36@mail.ru

There are only three solid planet-satellite pairs in the Solar system: Earth – Moon, Mars – Phobos, Pluto – Charon. For the first two pairs tectonic analogies were shown and explained by moving them in one circumsolar orbit. As it is known from the wave planetology [3, 4, 6] , "orbits make structures". For the third pair the same was stated as a prediction based on this fundamental rule. Global tectonic forms of wave origin appear in cosmic bodies because they move in keplerian orbits with periodically changing accelerations. Warping bodies waves have a stationary character and obeying wave harmonics lengths. Starting from the fundamental 2πR- long wave 1 making the ubiquitous tectonic dichotomy (two-face appearance) warping wave lengths descend along harmonics. Very prominent along with the wave 1 are waves 2 responsible for tectonic sectoring superimposed on the wave 1 segments. Practically all bodies have traces of shorter waves making numerous polygons (rings) often confused with impact craters.

Earth and the Moon moving in one circumsolar orbit both are distorted by wave 1, wave 2 and wave 4 features aligned along extent tectonic lines [4, 5]. At Earth they are: Pacific Ocean (2πR-structure) and Indian Ocean (πR-structure) from both ends with Malay Archipelago (πR/4-structure) in the middle. At Moon they are: Procellarum Ocean (2πR) and SPA Basin (πR) from ends and Mare Orientale (πR/4) in the middle. A regular disposition is surprising. Both Oceans and Basin occur on opposite hemispheres, lying in the middle both ring structures occur in the boundary between two hemispheres and are of the same relative size. These triads stretch along lines parallel to the equator (Earth) and with the angle about 30 degrees to it (Moon) indicating at a different orientation of the rotation axes in the ancient time [2]. On the whole, one could speak about a "lunar mould" of Earth [5] (Fig. 1-3).

Another tectonic twin is the pair Mars – Phobos. Both bodies sharing one circumsolar orbit, twice as long as the Earth – Moon orbit, acquire slightly oblong ellipsoidal shape (Fig. 4, 5). Very pronounced on both so much different in size and composition bodies the deepest basins – Hellas and Stickney (sectoral πR-structures) are comparable features.

The structural unity is predicted also for the third solid body pair – Pluto – Charon.

References: [1] Andrews-Hanna, J.C., Besserer, J., Head III, J.W. et al. 2014b. Structure and evolution of the lunar Procellarum region as revealed by GRAIL gravity data. Nature, v. 514, #7529, 2014, 68-71, doi: 10.1038/nature 1369; **[2]** Garrick-Bethell, I., Perera, V., Nimmo, F., and Zuber, M.T. 2014. The tidal-rotational shape of the Moon and evidence for polar wander. Nature, v. 512, issue 7513, 14 Aug. 2014, 181-184; **[3]** Kochemasov G.G. Theorems of wave planetary tectonics. Geophys. Res. Abstr. 1999. V.1, №3, P.700; **[4]** Kochemasov G.G. Earth and Moon: similar structures – common origin // NCGT Journal, 2014, v. 2, # 2, 28-38; **[5]** Kochemasov G.G. A lunar "mould" of the Earth's tectonics: four terrestrial oceans and four lunar basins are derivative of one wave tectonic process // NCGT Journal, v. 3, # 1, March 2015, 29-33; **[6]** Kochemasov G.G. Ceres' two-face nature: expressive success of the wave planetology // NCGT Journal, v. 3, # 1, March 2015, 63-64; **[7]** Oberst, J., Shi, X., Elgner, S., Willner, K. 2014. Dynamic shape and down-slope directions on Phobos. The fifth Moscow Solar system symposium. Space Research Institute (IKI) RAS, 13-18 October 2014, Abstract 5MS3-MS-11.

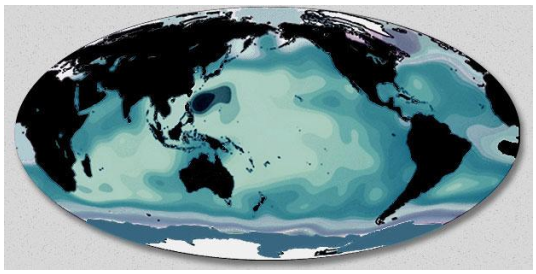

Fig. 1, 2.

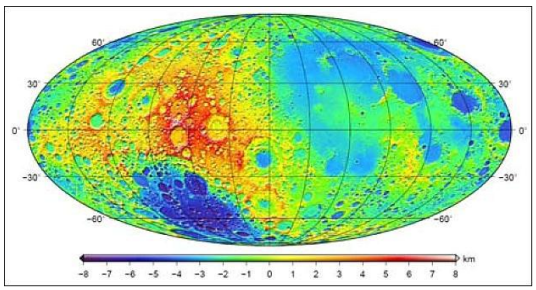

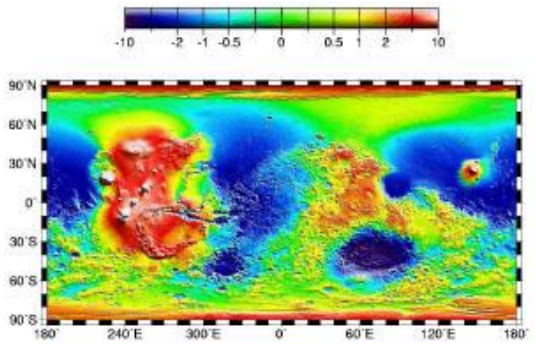

Fig. 4 (above) and Fig. 5.

Fig. 3.

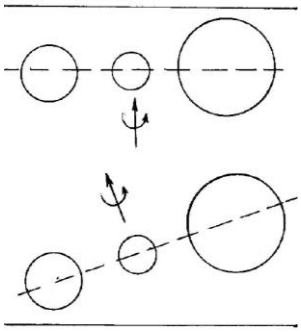

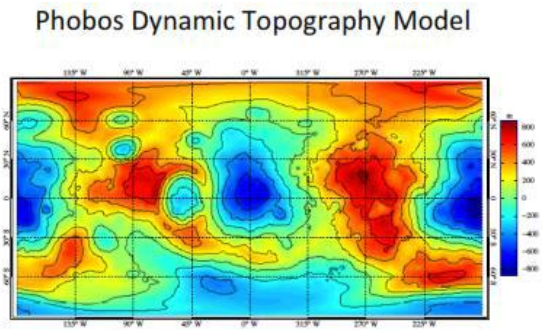

Fig. 1, 2. Earth's oceans; Lunar topography; **Fig. 3.** Schematic sizes and relative dispositions of terrestrial (above) and lunar wave born tectonic features. Pacific Ocean and Procellarum Ocean at the right - 2πR structures. Indian Ocean and SPA Basin on the left– πR structures. Malay Archipelago and Mare Orientale at the center – πR/2 structures. Equators (axis of rotation) positions at present (Earth) and at ancient Moon; **Fig. 4, 5**. Mars (above) and Phobos topography [7]. Global tectonic parallel.

EPSC Abstracts
Vol. 10, EPSC2015-92, 2015
European Planetary Science Congress 2015

Virtual planets atlas 1.0 freeware

Christian Legrand[1] and Patrick Chevalley[2], [1]Software designer / Ch. Legrand 668 Rue du Tour de Préaux 76160 PREAUX (France) / chlegrand76@hotmail.fr , [2] Software programmer / P. Chevalley 160 Route d'Aire CH-1219 AIRE (Switzerland) / pch@ap-i.net.

1. Introduction

Since 2002, we develop the "Virtual Moon Atlas - http://www.ap-i.net/avl/en/start" a freeware to help Moon observing and to improve interest for Moon in general public. VMA freeware has been downloaded near 900 000 times all over the world and is or has been used by several professional organizations such as Kitt Peak Observatory, National Japan Observatory, Birkbeck College / University College London (K. Joy), BBC Sky at night, several French astronomy magazines and astronomy writers (P. Harrington, S. French…) . Recommended by ESA, registered as educational software by French ministry for education, it has also yet been presented at 2006 & 2007 LPSC and PCC2 in 2011

We have declined this freeware in a new tool with the same goals, but for the telluric planets and satellites, the "Virtual Planets Atlas (VPA / http://www.ap-i.net/avp/en/start") now in version 1.0.

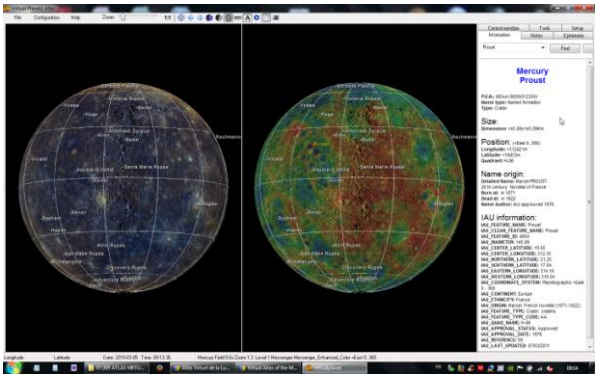

Picture 1 : VPA 1.0 main screen : Mercury with Messenger enhanced colors overlay (left) and Messenger altitude overlay (left) and selected feature information thumbnail.

2. Presentation

VPA uses datas coming from IAU nomenclatures, NASA & ESA planetary missions, USGS & JPL mapping works and from Dr Stooke personal work. First version is about Mercury, Venus & Mars.

The software includes, for each planet, the management of a complete database (Derived from official IAU nomenclatures) of named features of these Solar System bodies.

VPA 1 is presently available for Windows, Linux and Mac 0S. Two languages are now used (EN & FR), but we plan to translate software interface in all major other languages (GE / SP / IT / CN…) .

2.1 Software features :

- « Map » window with various functions thumbnails as « Information », « Ephemeresis », « Notes», « Tools », « Setup», …
- Full rotating planets globe with coordinates grid
- Second window ability permitting comparisons between different textures and overlays.
- Real time or chosen phases seen from Earth display
- Orientation of the planet disk with powerful zoom
- Formations search function starting from name
- Formations names display related to zoom power
- Integrated notepad for your own notes on formations
- Size and distance measurement tool on maps
- Context menu on right mouse click
- Maps and databases printing with captions setup
- Full screen display for public videoprojections

2.2 Databases :

Included databases contains presently more than 4 000 formations:

- 401 formations nommées pour Mercure
- 2033 formations nommées pour Vénus
- 1797 formations nommées pour

For each formation, IAU official datas are translated.

All these databases include the "PUN / Planetary Universal Number" conceived by ourselves and permitting to "name" and localize any formation more than 1arc minute wide.

2.3 Mapping textures :

Mercury : B&W Messenger (0.5 km / Pix)
Venus : B&W Magellan (1 km / Pix)
Mars : Color Viking (0.8 km / Pix)
Others new planets and satellites textures planned for the end of 2015.

2.4 Historical textures : Permitting easy comparison of these pioneer works with present datas : > Lowell / Schiaparelli / Dolfuss / Arecibo / Mariners / Hubble ST…

2.5 Scientific overlays : More than 30 different: (Gravity, temperature, altimetric, geologic, various chemical elements …) overlays that can be applied on or without each texture.

2.6 Delivery : VMA Pro 6 version and all add-ons collection are freeware and downloadable free from our Web site http://www.ap-i.net/avl/en/start
We maintain a discussion forum and encourage other languages translations. We also listen continuously to our users requests, (including professionals), to update new useful functionalities.

Acknowledgements

Sincere thanks to Dr Phil Stooke of the Western University of Canada for authorizing us to use his work and to Emily Lakdawalla of the Planetary Society for her support to our project. We also thank IAU, LPI, LPL, NASA and ESA for releasing useful planetary datas to public domain.

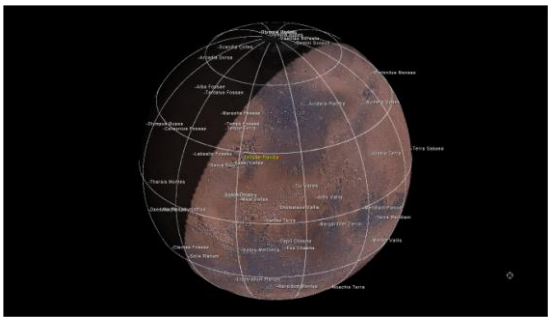

Picture 4 : Full screen for public education events

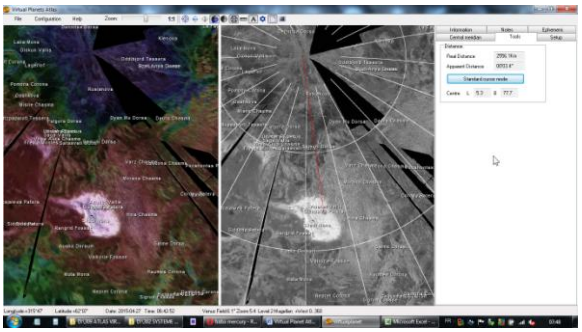

Picture 5 : Venus Maxwell Montes with altitude and distance to North Pole measurement

Picture 6 : Mars revised geological overlay.

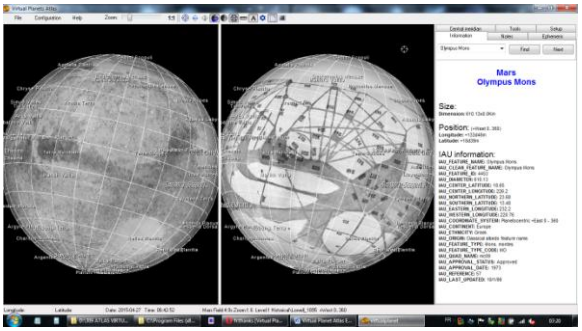

Picture 7 : MRO vs Lowell 1895 textures

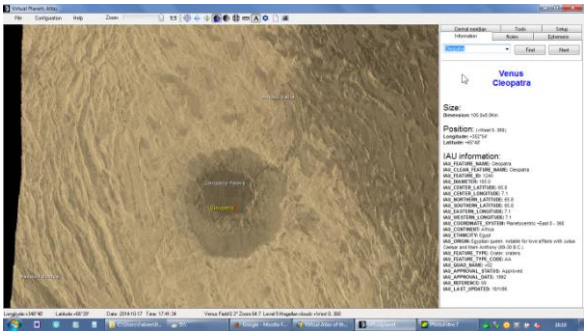

Picture 8 : Venus MRO colored Cleopatra crater

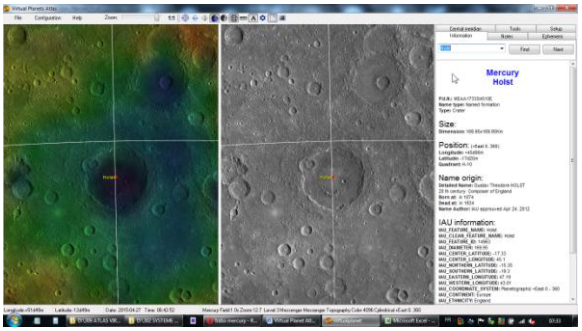

Picture 7 : Mercury Holst Topography & MRO

EPSC Abstracts
Vol. 10, EPSC2015-118, 2015
European Planetary Science Congress 2015

Gravity effects on sediment sorting: limitations of models developed on Earth for Mars

N.J. Kuhn (1), B. Kuhn (1) and A. Gartmann (2)
(1) Physical Geography, Environmental Sciences, University of Basel, Switzerland, (2) Meteorology, Climatology, Remote Sensing, Environmental Sciences, University of Basel, Switzerland (nikolaus.kuhn@unibas.ch) / Fax: +41 61 267 07 40)

Abstract

Most studies on surface processes on planetary bodies assume that the use of empirical models developed for Earth is possible if the mathematical equations include all the relevant factors, such as gravity, viscosity and the density of water and sediment. However, most models for sediment transport on Earth are at least semi-empirical, using coefficients to link observed sediment movement to controlling factors such as flow velocity, slope and channel dimensions. However, using roughness and drag coefficients, as well as parameters describing incipient motion of particles, observed on Earth on another planet, violates, strictly speaking, the boundary conditions set for their application by fluid dynamics because the coefficienst describe a flow condition, not a particle property. Reduced gravity affects the flow around a settling partcile or over the bed of a watercourse, therefore data and models from Earth do not apply to another planet. Comparing observations from reduced gravity experiments and model results obtained on Earth confirm the significance of this error, e.g. by underestimating settling velocities of sandy particles by 10 to 50% for Mars when using models from Earth. In this study, the relevance of this error is examined by simulating the sorting of sediment deposited from water flowing on Mars. The results indicate that sorting on Mars is less pronounced than models calibrated on Earth suggest. This has implications for the selection of landing sites and, more importantly, the identification of strata potentially bearing traces of past life during rover missions on Mars. try, 2001.

EPSC Abstracts
Vol. 10, EPSC2015-154, 2015
European Planetary Science Congress 2015

Data preprocessing and preliminary results of the moon-based ultraviolet telescope on CE-3 lander

Wang,F.,Wen,W.-B., Xiao,Y., Zhao,S., Li,H.-Y., Fu,Q., and Liu,Y.-Y.
Key Laboratory of Lunar and Deep Space Exploration, National Astronomical Observatories, Chinese Academy of Sciences，Beijing, China (wangf@bao.ac.cn / Fax: +86-010-64888703)

Please make sure that your pdf conversion results in a document with a page size of 237 x 180 mm!

Abstract

The moon-based ultraviolet telescope (MUVT) is one of the payloads on the Chang'e-3(CE-3) lunar lander. Because of the advantages of having no atmospheric disturbances and the slow rotation of the Moon, we can make long-term continuous observations of a series of important remote celestial objects in the near ultraviolet band, and perform a sky survey of selected areas. We can find characteristic changes in celestial brightness with time by analyzing image data from the MUVT, and deduce the radiation mechanism and physical properties of these celestial objects after comparing with a physical model. In order to explain the scientific purposes of MUVT, this article analyzes the pre-processing of MUVT image data and makes a preliminary evaluation of data quality. The results demonstrate that the methods used for data collection and preprocessing are effective, and the Level 2A and 2B image data satisfy the requirements of follow-up scientific researches.

1. Introduction

The moon-based ultraviolet telescope(MUVT) system is used to observe galaxies, binary stars, active galactic nuclei and bright stars. It is the first long-term observatory to be deployed on the Moon.

The MUVT system covers a wavelength range of 245 to 340 nanometers. It consists of a Ritchey-Chretien telescope(RCT). It uses a pointing mirror that features a two-dimensional gimbal to track objects.

The Chang'e-3(CE-3) lunar probe was launched on 2013 December 2 from the Xichang Satellite Launch Center. It made a successful soft landing on the Moon on December 14. The CE-3 probe landed in Mare Imbrium, 44 degree north of the lunar equator. The MUVT is mounted in the cabin–Y of the Lander. Therefore, the best option for the scientific observation is in a direction near north celestial pole.

From 2013 December 16 to now, a series of scientific explorations by the MUVT has been carried out in sequence, including: instrument calibrations, shafting observations that calculate the direction of the optical path in celestial coordinates, surveys, pointing observations.

2.Data preprocessing and preliminary results

The flowchart of the MUVT data preprocessing mainly includes the following steps: First, data communication channel processing includes: frame synchronization, Reed-Solomon decoding and optimized selection of two possible ground stations; Second, the frame data are compartmentalized and subcontracted; then, the extraction of the MUVT source packet data; label data from different Earth days into data blocks, after physical conversion; Level 2A data processing is related to instrument correction; level 2B data produce the results for processing related to identifying location.

The following mainly concerns with how the preprocessing method is related to level 2A and level 2B data products and preliminary results.

Because the moon-based ultraviolet telescope system works in the lunar day, and sunshine is the main source of stray light. To remove the contamination due to stray light is key. At first, we group images in each observational run by their pointing. The pattern of stray light in a given image is constructed by combining all the images(except the given image) in the group. Contamination from stray light is

subsequently removed from a given image by subtracting the constructed pattern of stray light.

On the ratio analysis of the starlight concentration, the target star, fitting the light distribution by a 1-dimensional Gaussian returns a FWHM of the pixels, which indicates that more than 80% energy is enclosed within 3 x 3 pixels for a point source.

The AB magnitude system is adopted by MUVT. Basing upon the observations of the standard star HD188665 (spectral type B5V) at the beginning the MUVT mission and the date reduction described above, we obtained a preliminary results on the magnitude zero point of Z=17.49 ± 0.02 mag, in which the error corresponds to 1sigma significance level and is obtained from multiple observations. Fig. 1 shows the results in the condition that a goal star is repeated sampling with the same aperture and the parameters. The magnitude diffusion of 1 σ by aperture photometry is 0.06 magnitude.

3. Figures

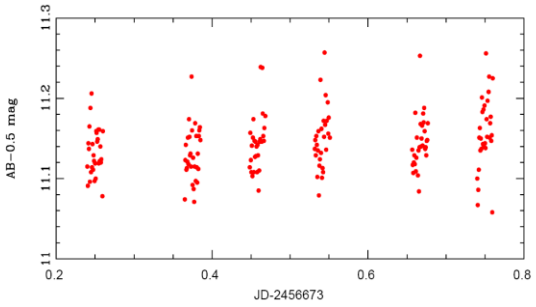

Figure 1: The dispersion analysis for the target by multiple sampling.

6. Summary and Conclusions

The MUVT is one of the payloads equipped on the lander. This is the first time the continuous monitoring of important optical variables and surveys of an area with low galactic latitude have been performed. It has worked at least half and one years in accordance with the design life of the instrument on the Moon. The MUVT operates in three modes: standby mode, the state of being powered on but not collecting data; adjusting mode, the state where adjustments and pointing are made; detection mode, saving data received while the device is operating. Through the analysis of data products from the first and second lunar days, instrument correction and stray light reduction are performed for all images, so the effects of the instrument and stray light are effectively removed. According to the results of data analysis, the instrument could observe magnitude 13 stars(with an SNR of 5) in a 30s exposure during the Moon's twilight period. However, at about lunar noon, due to the interference of stray light from the sun, the observation capacity is reduced to about magnitude 11(with an SNR of 5). The preprocessing method is reasonable and the data products are effective. All data products can be used as the data base of scientific research on ultraviolet astronomical observation.

Acknowledgements

We wish to thank all members from the Ground Research and Application System and the Moon-based Ultraviolet Telescope instrument group(Key Laboratory of Space Astronomy and Technology) that is part of the Chang'e-3 program, whose joint efforts have made the data acquisition and preprocessing used for this study possible.

References

[1] Tan X., Liu J. J., Li C. L., et al. 2014, Research in Astron. Astron. Astrophys. (RAA), 2014.

[2] Cao Li, Ruan Ping, Cai HongBo et. LUT: A Lunar-based Ultraviolet Telescope, 2011 (In Science China).

[3] Jia Yingzhuo. The report of the CE3' payload flight model, 2011.

[4] Cao Li. The calibration summary report of the moon ultraviolet telescope, one of the CE-3' payloads. 2012.

[5] J. Wang, J. S. Deng, J. Cui et: Lunar exosphere influence on lunar-based near-ultraviolet astronomical observations, 2011 (In Adv. Space Res.).

[6]Ip,W.-H.,Yan,J.,Li,C.-L.,&Ouyang,Z.-Y.,2014,RAA(Research in Astronomy and Astrophysics),14,1511

EPSC Abstracts
Vol. 10, EPSC2015-234, 2015
European Planetary Science Congress 2015

Effects of giant impacts on the mantle and atmosphere of terrestrial planets at medium and long time scales.

C. Gillmann (1), G. Golabek (2) and P. Tackley (3)

(1) Royal Observatory of Belgium, Belgium, (2) University of Bayreuth, Germany (3) University ETHZ, Switzerland (cedric.gillmann@observatoire.be)

Abstract

Our main interest is to understand how surface conditions change during a planet's evolution and which mechanisms are most important. Therefore, we investigate how the coupled evolution of Venus' atmosphere and mantle is modified by giant impacts. We focus on volatile fluxes in and out of the atmosphere: atmospheric escape and degassing. We link those processes into a coupled model of mantle convection and atmospheric evolution. Feedback of the atmosphere on the mantle is included via surface temperature. As large impacts are capable of contributing to atmospheric escape, volatile replenishment and energy transfer, we estimate their effects on the evolution of Venus.

1. Introduction

The study of terrestrial planets' surface conditions and their evolution with time is necessary to understand how and when a planet becomes habitable. Recently, perception of the importance of interactions between interior and exterior has led to better understanding of the evolution of planets [1, 2, 3]. Due to its activity and dense atmosphere, Venus is a perfect place to test models. While it has similar general characteristics to Earth, conditions at its surface are very different, with an average surface temperature of around 740 K, due to its 92 bar CO_2 atmosphere. The solid part of the planet could still be active [4, 5]. Additionally, it is generally thought that, based on crater counting, the surface of Venus is relatively young. Our understanding of the formation and early evolution of the solar system and observation of its terrestrial bodies shows that impacts are unavoidable. Giant collisions, in particular are suspected to have strong effects on the surface conditions of terrestrial planets. We want to understand how they can affect a Venus-like planet.

2. Model

The model can be separated into four different parts.

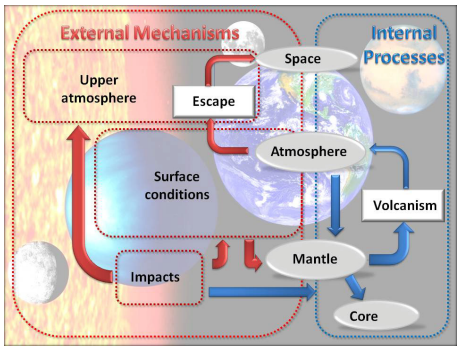

Figure 1: basic layout of the model.

(i)Internal processes are dependent on mantle dynamics. We use a variation of the StagYY code designed for Venus [6]. Physical are depth-dependent. The phase transitions in the olivine system and in the pyroxene-garnet system are included. The assumed rheology is Newtonian diffusion creep plus plastic yielding. Degassing is calculated when melting occurs and we use a wide range of possible lava compositions (10-300 ppm for water, 5-5000ppm for CO_2).

(ii)Atmospheric escape modeling involves two different aspects: hydrodynamic escape (0-500 Myr) and non-thermal escape mechanisms (dominant post 4 Ga). Hydrodynamic escape is the massive outflow of light volatiles into space occurring when the solar energy input (Extreme UV and solar wind) is strong. Post 4 Ga escape from non-thermal processes is comparatively low. It is also powered mainly by EUV. Mechanisms include sputtering, ion pick-up, plasma clouds and dissociative recombination. Constraints include present-day measurements by the ASPERA instrument and recent numerical simulations.

(iii) Surface conditions are calculated from the greenhouse effect of main gases from the atmosphere: water and CO_2. We use a one-dimensional radiative-convective grey atmosphere model modified from [1]. Surface temperature is thus calculated and used in the mantle convection model as a boundary condition.

(iv)Impacts can bring volatiles and erode the atmosphere. Mantle dynamics are modified by the large amount of energy brought to the mantle. A thermal anomaly created by the impact is used and can lead to melting. Volatile evolution due to impacts is heavily debated so we test a broad range of impactor parameters (size, velocity, timing) and test different impact erosion factors.

3. Results

We are able to produce models leading to present-day-like conditions through episodic volcanic activity consistent with Venus observations (eruption rates, present-day state, possible resurfacing events). Changes in water vapor partial pressure lead to variations in surface temperatures of up to 200 K during, which have been identified to have an effect on volcanic activity. We note a clear correlation between low temperature and mobile lid regime.

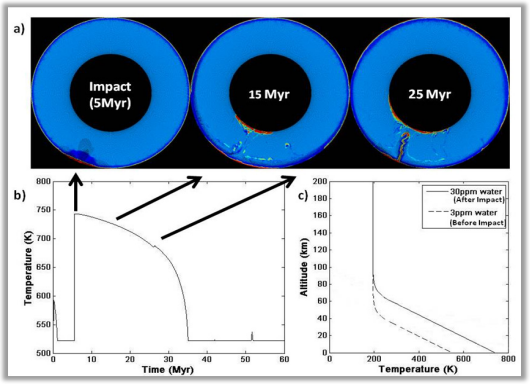

Figure 2: short term effects of a large impact.

We observe short term and long term effects of the impacts on planetary evolution. Single impact atmosphere erosion affects evolutions only in a marginal way, even for massive (up to 800 km) impacts. For volatile balance, smaller (less than 50 kilometer scale) meteorites have a negligible effect. Larger ones (from 100 km up) generate melt both at the impact and later on, due to volcanic events they triggered. A significant amount of volatiles can be released on a short timescale.

Truly massive impacts (400+ km) can even have global and billion years scale consequences, especially when they occur at specific times.

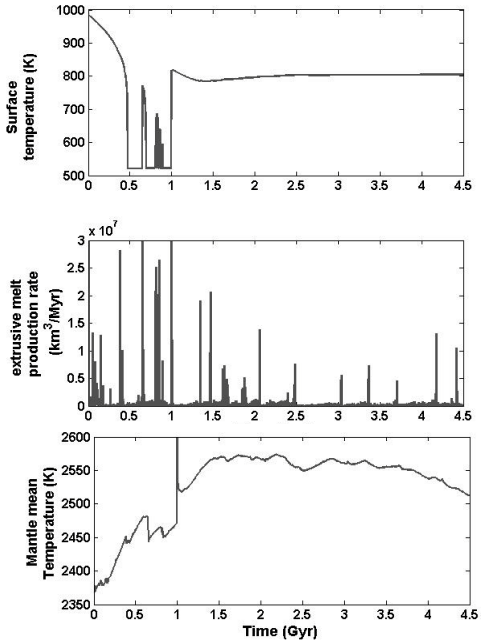

Figure 3: Long term evolution of Venus with a 400 km impact 3.5 Ga ago.

Early impacts can deplete much of the initial volatile content of the mantle, leading to low later degassing if the mantle is not replenished (subduction).
Later impact can counteract the effect of atmosphere escape by releasing volatile into the atmosphere at a larger rate than volcanism in a single event. The resulting high surface temperatures affect directly mantle convection pattern and can prevent mobile lid regime from initiating, with profound consequences for volatile exchanges and mantle evolution.

References

[1] Phillips, R.J., et al. Climate and interior coupled evolution on Venus. Geophys. Res. Lett. 28, 2001. **[2]** Gillmann, C. and Tackley, P., Atmosphere/mantle coupling and feedbacks on Venus, JGR Planets, 2014. **[3]** Noack, L., et al., Coupling the Atmosphere with Interior Dynamics: Implications for the Resurfacing of Venus, Icarus 2012. **[4]** Bullock, M.A., Grinspoon, D.H., The recent evolution of climate on Venus. Icarus 150, 2001. **[5]** Smrekar, S. E., et al., Recent Hotspot Volcanism on Venus from VIRTIS Emissivity Data. Science 328, 2010. **[6]** Armann, M., and P. J. Tackley, Simulating the thermochemical magmatic and tectonic evolution of Venus's mantle and lithosphere: Two-dimensional models, J. Geophys. Res., 2012.

EPSC Abstracts
Vol. 10, EPSC2015-289, 2015
European Planetary Science Congress 2015

Statistical analysis of the Martian surface

F. Landais(1), F. Schmidt (1), S. Lovejoy (2)
(1) Univ Paris-Sud/CNRS, GEOPS, UMR8148, Orsay, F-91405, France, (francois.landais@@u-psud.fr)(2) Physics, McGill University, Montreal, Quebec

Abstract

We investigate the scaling properties of the topography of Mars [10]. Planetary topographic fields are well known to exhibit (mono)fractal behavior. Indeed, fractal formalism is efficient to reproduce the variability observed in topography. Still, a single fractal dimension is not enough to explain the huge variability and intermittency. Previous study have shown that fractal dimensions might be different from a region to another, excluding a general description at the planetary scale. In this project, we are analyzing the Martian topographic data with a multifractal formalism to study the scaling intermittency. In the multifractal paradigm, the local variation of the fractal dimension is interpreted as a statistical property of multifractal fields. The results suggest a multifractal behaviour from planetary scale down to 10 km. From 10 km to 600 m, the topography seems to be simple monofractal. This transition indicates a significant in the geological processes governing the Red Planet's surface.

1. Introduction

The acquisition of altimetric data from Mars Orbiter Laser altimeter (MOLA) has motivated numerous analysis of the martian topography, in particular the surface roughness. A possible approach is to assume that topography can be mathematically described as a statistical field with quantitative parameters able to characterize the geologiccal units. Many statistical indicators have been proposed and widely explored in order to study the surface of Mars: RMS height, RMS slope, median slope [1], autocorrelation length [2]. Usefull informations have been obtained by the use of those indicators but they have the disadvantage of been defined at a given scale. By construction, they do not directly take into account the well-established scale symmetry that generally occurs in the case of natural surfaces. Indeed, topography can not be interpreted as a stationary field, meaning that statistical parameters like the mean or the standard deviation exhibit a dependence toward scales. Hence the nature of this dependence needs to be accurately explained, otherwise the description of the surface remain incomplete. This subject has been widely studied in the past, parallel to the development of the notion of fractals ([3]). It is now well established that topography is efficiently modelled by fractal simulations. More interestingly, the fractal theory provides a mathematical formalism to describe the scale dependence of statistical parameters toward scales. It turns out that simple power-law relations efficiently approach the variability of planetary surfaces. The associated power-law exponent provides a quantitative parameter that is a good scale-independent candidate to characterize the geometric properties of a natural surface. A common example is given by the power spectrum of topographic field providing roughness information in the frequency space.
On Mars, different authors have explored the scaling properties of topography by the use of scale invariant parameters. The observed intemittency [4] apparently rejects the idea of a global description of any topographic field at the planetary scale. However, modern developments in the fractal theory might be able to give full account to the observed variability and intermittency. As proposed by [5], it is possible to extent the fractal interpretation of topography to a multifractal statistical object requiring an infinite number of fractal dimensions (one for each statistical moment).

2. Data and method

We used the MOLA instrument database to study Mars [6]. The absolute vertical accuracy is ~10 m but depends on accuracy of reconstruction of radial spacecraft orbit. The surface spot size is 130 m. The along-track point spacing is 330 m. The across-track shot spacing depends on mapping orbit and vary with latitude since the orbit is quasi-polar.
The MOLA topography database is available in the PDS archive. This database has been filtered from

noise and atmospheric clouds reflectors. We used the MOLAUtils tools developed to extract all the points in a given surface [7].

The haar fluctuations [8] are computed for all the available along-track points on the MOLA database and splitted in 74 bins of scale form 600m to the planet scale. For each bin of scales, 21 statistical moment are computed (order 0.1 to 2, step 0.1).

3. Results

Figure 1 is the main result of this analysis. Although the linear correlation (scaling) is satisfying, two distinct scaling regimes occur with a transition around 10 km. Figure 2 presents the slope of the linear fit for different moments (blue point : <10km, red points : >10km).

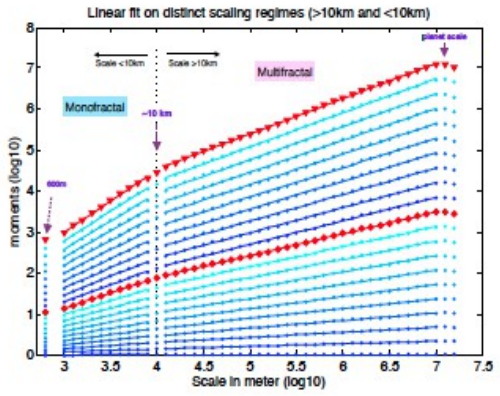

Figure 1: Linear fit on the two different scaling regimes (inferior and superior to 10 km) for every 21 statistical moments from 0.1 to 2.

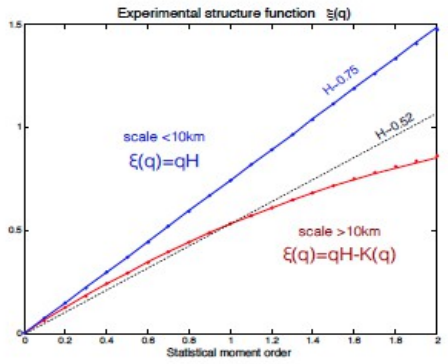

Figure 2: Theoretical structure function ς(q) combining the 21 linear fits shown on figure 1. Red points (resp.blue points) correspond to the range of scales superior (resp. inferior) to 10km

4. Discussion and conclusion

Multiscaling seems to occur on a large but restricted range of scale (superior to 10 km) with a Hurst exponent H = 0.52. At smaller scale, the topography is still scaling but the symmetry is only monofractal with a parameter H = 0.75.

We demonstrate that a change of processes governing the Martian topography occurs at 10 km. A multiplicative cascade process is occurring at scale higher than 10 km but a simpler monofractal scaling process is occurring a small scale. Craterisation is well known to be a fractal process with a single fractal dimension ([9]). We propose that the low scales are dominated by craterisation processes, at the origin of the monofractal scaling law. This process has already been proposed by [1]. Future investigations are required to understand the multiplicative cascade processes at large scale

References

[1] Oded Aharonson, Maria T. Zuber, and Daniel H. Rothman, JGR : Planets, 106(E10):23723–23735, 2001. [2] Mikhail A. Kreslavsky and James W. Head. JGR: Planets, 105(E11):26695–26711, 2000 [3] Benoit Mandelbrot, Science ,156(3775):636–638, 1967. [4] R. Orosei, R. Bianchi, A. Coradini, S. Espinasse, C. Federico, A. Ferriccioni, and A. I. Gavrishin. JGR: Planets , 108, 2003 [5] Shaun Lovejoy and Daniel Schertzer, JGR: Atmospheres , 95(D3):2021–2034, 1990. [6] David E. Smith et al, JGR: Planets, 106(E10):23689–23722, 2001. [7] http://planeto.geol.u-psud.fr/MOLAutils,50.html?lang=en [8] S. Lovejoy and D. Schertzer. NPG 19(5):513–527, 2012. [9] Margaret A. Rosenburg, Oded Aharonson. JGR: Planets, 2015. [10] Landais, F. et al., Non-Linear Processes in Geophysics, submitted

EPSC Abstracts
Vol. 10, EPSC2015-431, 2015
European Planetary Science Congress 2015

Origin and nature of intercrater plains in northwestern rim of Hellas Basin

F. Salese (1,7,8), N. Mangold (2), V. Ansan (2), J.Carter (3,4), A. Ody (5), F. Poulet (3) and G.G. Ori (1,6,7)

(1) International Research School of Planetary Sciences, Università "G. d'Annunzio", Viale Pindaro 42, 65127 Pescara, Italy, francesco.salese@unich.it; (2) Laboratoire de Planetologie et de Geodynamique de Nantes, CNRS/Nantes University, France; (3) Institut d'Astrophysique Spatiale, Université Paris Sud 11, Bâtiment 121, 91405 Orsay, France; (4) European Southern Observatory, Vitacura, Santiago, Chile; (5) Laboratoire de Géologie de Lyon: Terre, Planètes, Environnement, Université de Lyon 1 (CNRS, ENS-Lyon, Université de Lyon), rue Raphaël Dubois 2, 69622 Villeurbanne, France; (6) Ibn Battuta Centre, Université Cady Ayyad, Marrakech, Morocco; (7) Dipartimento di Ingegneria e Geologia, Università d'Annunzio, Viale Pindaro, 42, 65127 Pescara (PE), Italy; (8) INAF-OACTe, Istituto Nazionale di Astrofisica, Osservatorio Astronomico di Teramo, Italy.

1. Introduction

The nature and origin of intercrater plains within the martian cratered highlands is a major unresolved and controversial issue that have been somewhat enigmatic, receiving little attention since the Mariner era [1,2,3,4,5]. Are flat-lying smooth plains sedimentary or volcanic or both ? Whether these plains are mainly constituted of volcanic material or sediments is a crucial difference for understanding the surface environment of the Noachian period. In order to answer to previous question, we focus our study on the NW rim of Hellas basin defining first the relative stratigraphy and absolute age, throughout crater counting method, of the different units by a precise mapping and correlating then these units with mineralogy and texture.

Hellas region is a key because of the possibility to constrain these processes geographically and temporarily, including the presence of erosional windows, which is a key for enabling this work to distinguish the origin of layering. The study area could be of particular interest to the question of habitability. Indeed, there is the possibility that a variety of aqueous systems, in particular marine/lacustrine [6] and hydrothermal systems [7], may have formed in the region after the Hellas impact.

2. Data and methods

Visible light and thermal imagery was used for texture and stratigraphy from CTX (ConTeXt camera), HiRISE (High Resolution Imaging Science Experiment), HRSC (High Resolution Stereo Camera), THEMIS (Thermal Emission Imaging System) instruments. OMEGA (Observatoire pour la Minéralogie, l'Eau, les Glaces et l'Activité) and CRISM (Compact Reconnaissance Imaging Spectrometers for Mars) data were used for detailed mineralogical analysis. Correlation between mineralogy, stratigraphy and texture is key in connecting together units and conclude for their origin.

Consistent with the approach that [8] applied to planetary mapping, we identify and map rock units and sedimentary cover on the basis of their apparent geologic uniqueness as defined by their primary physical features, areal extent, relative age, and geologic associations.

Primary features, including layering, albedo, and thermophysical character, formed during emplacement; whereas secondary features, including craters, ridge and valley networks or channels, are formed after emplacement. In many cases, especially in the presence of ghost, eroded craters or old ejecta, delineating primary and secondary features requires careful observation and may be difficult where overprinting of secondary features has masked, obliterated, or mixed with primary features. Units are primarily identified and delineated based on geologic relationships and relative ages. We determine the age of different units based on crater counting.

3. Preliminary Results

Hellas basin is characterized by the interaction between volcanism and sedimentary deposition as reconstructed by our geological map. The rim of the northern Hellas basin shows a complex geological history. There are sedimentary plains from which remnant buttes (ancient Hellas) standing up and locally crosscut/mantled by younger volcanic lava flows. We identify four kinds of deposits: bedrock, ejecta sedimentary and volcanic deposits. We focus our attention on intercrater plains and more specifically our analysis on sedimentary and volcanic deposits. Volcanic deposits are characterized by high thermal inertia in THEMIS nighttime images (Fig. A), rough surfaces (Fig. C) at CTX scale and they do not overlap high standing buttes (Fig. B).

Sedimentary deposits are characterized by low thermal inertia in THEMIS nighttime images (Fig. A) except for erosional windows with fresh material outcropping. They show very high thermal inertia, smooth surfaces (Fig. D) at CTX scale and they drape the morphologies. We use erosional windows and shoulder of fresh impact crater as natural cross-cutting section to reconstruct the stratigraphy of the studied area as shown in Fig. E, F, G. The analysis of crater statistics and derivation of crater model ages shows that sedimentary units were deposited at the end of the Noachian period whereas the volcanic unit represents a resurfacing event dated in the Hesperian. Sedimentary units drape bedrock hills postdating them.

Conclusions

These new data show a more complex geological history of northeastern rim of Hellas region. Our geological map reveals many previously unrecognizable units, features, and temporal relations. The presence of many sedimentary deposits question their origin as part of the sedimentary systems observed locally in Terby crater [9], linking the eroded region of Tyrrhena Terra to the putative paleolake inside Hellas Basin. Further work will attempt to correlate the geological units mapped with the mineralogy obtained from orbital spectrometers.

References

[1] Malin, M. C. (1976), Ph.D. dissertation, 186 pp., Calif. Inst. of Technol., Pasadena. [2] Malin, M. C., and D. Dzurisin (1977), *Journal of Geophysical Research*, 82(2), 376-388. [3] Greeley, R., and P. D. Spudis (1981), Volcanism on Mars, *Reviews of Geophysics*, *19*(1), 13-41. [4] Tanaka, K. L., and P. A. Davis (1988), *Journal of Geophysical Research: Solid Earth (1978–2012)*, *93*(B12), 14893-14917. [5] Edgett, K. S., and M. C. Malin (2002), *Geophysical Research Letters*, 29(24), 32-31-32-34. [6] Wilson, S. A. et al., (2007), *Journal of Geophysical Research: Planets* (1991–2012), 112(E8). [7] Newsom, H. E. (1980), *Icarus*, 44(1), 207-216. [8] Hansen, V. L. (2000), *Earth and Planetary Science Letters*, 176(3), 527-542. [9] Ansan, V., D. et al., (2011), *Icarus*, 211(1), 273-304.

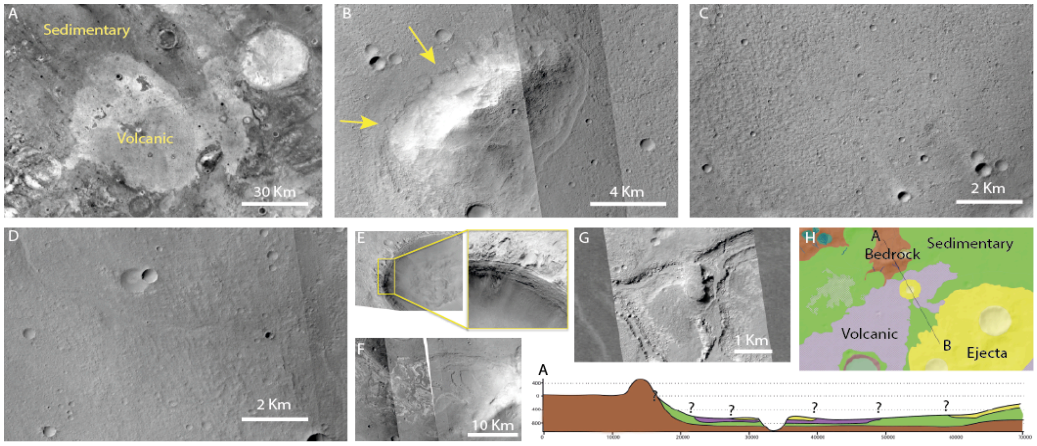

Figure A) THEMIS nighttime image shows sedimentary and volcanic deposits having respectively low (dark) and high (white) thermal inertia; B) Yellow arrows indicate that volcanic deposits don't drape the morphology; C) Particular of rough surface of volcanic deposit; D) Particular of smooth surface of sedimentary deposit; E) Shoulder of fresh impact crater in sedimentary deposits showing in the inset well stratified sedimentary deposits; F/G) Erosional windows in sedimentary deposits showing well stratified and laterally continuous sedimentary deposits. At CTX and HiRISE scale respectively; H) Example of geological map and stratigraphic profile of the study area.

EPSC Abstracts
Vol. 10, EPSC2015-572, 2015
European Planetary Science Congress 2015

Influence of the radiation pressure on the planetary exospheres: density profiles, escape flux and atmospheric stability

A. Beth (1), P. Garnier (2,3), D. Toublanc (2,3), I. Dandouras (2,3), C. Mazelle (2,3)
(1) Dpt of Physics, Imperial College London, London, United Kingdom (a.beth@imperial.ac.uk)
(2) Université de Toulouse; UPS-OMP; IRAP; Toulouse, France
(3) CNRS; IRAP; 9 Av. colonel Roche, BP 44346, F-31028 Toulouse cedex 4, France

Abstract

The uppermost layer of the atmosphere, the exosphere, is not well-known in its global structure since the densities are very low compared to instrument detection capabilities. Because of rare collisions and high Knudsen numbers, the motion of light species (H, H_2, ...) in the corona is essentially determined by the external forces : the gravitation from the planet, the radiation pressure, as well the stellar gravity.
In this work, we calculate rigorously and analytically, based on the Hamiltonian mechanics and Liouville theorem, the impact of the radiation pressure and gravitation from the planet on the structure of the exosphere. This approach was partially used by Bishop and Chamberlain (1989) but only in the 2D case : we extend it to the 3D case. Assuming a collisionless exosphere and a constant radiation pressure near the planet, we determine the density profiles for ballistic particles (the main contribution for densities in the lower exosphere) for light species as a function of the angle with respect to the Sun direction. We also obtain an analytical formula for the escape flux at the subsolar point, which can be compared with the Jeans' escape flux.
Finally, we study the effect of the radiation pressure on the zero velocity curves, position of the Roche lobe and Hill's region for the well-known Three-Body problem especially for Hot Jupiters and discuss about the validity of our model. The goal is to bring some constraints on modelling of exoplanet atmospheres.

1. Introduction

The exosphere is the upper layer of the atmosphere where the densities are low compared to intrument detection capabilities. Thus, we need to model this part of the atmosphere to explain observations of densities or escape flux from exoplanet atmospheres.
In this region, the gas is directly in interaction with the interplanetary medium: the gas is subject to both planet and stellar gravities, scarse collisions and radiation pressure. We propose a way to model the escape flux, as well as the densities of one type of particles in a collisionless exosphere: the ballistic particles. These are linked to the planet by gravitation and not enough pushed away by the radiation pressure to escape.

2. Model and results

For this problem, we use a hamiltonian approach. In the presence of the radiation pressure and the gravitational force, the Hamiltonian is given by:

$$\mathcal{H} = \frac{p_r^2}{2m} + \frac{p_\theta^2}{2mr^2} + \frac{p_\phi^2}{2mr^2\sin^2\theta} - \frac{GMm}{r} + ma\cos\theta$$

where r is the distance from the planet, θ the angle between the particle and the Sun, ϕ the angle between the particle and the ecliptic plane, p_r, p_θ and p_ϕ are the conjugate momenta, a the constant acceleration due to the radiation pressure. It is then necessary to use a parabolic system of coordinates:

$$u = r(1+\cos\theta) \quad w = r(1-\cos\theta)$$

and the Hamiltonian becomes:

$$\mathcal{H} = \frac{2up_u^2 + 2wp_w^2}{m(u+w)} + \frac{p_\phi^2}{2muw} - \frac{2GMm}{u+w} + \frac{ma(u-w)}{2}$$

We define the Jeans parameter $\lambda(r) = GMm/k_BT_{exo}r$, $R_{pressure} = \sqrt{GM/a}$, $\lambda_c = \lambda(r_{exo})$ where r_{exo} is the distance of the exobase from the center of the planet and $\lambda_a = \lambda(R_{pressure})$.

Also, we estimate analytically the escape flux at the subsolar point including the effect of radiation pressure:

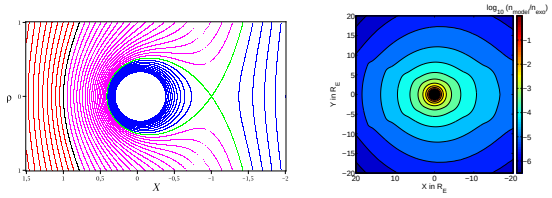

Figure 1: Zero velocity curves (dimension less distance) for our problem and ballistic particles density at Earth for hydrogen and $T_{exo} = 800\ K$

$$\mathcal{F} = \frac{n_{exo} U_{th}}{2\sqrt{\pi}} \frac{\lambda_c}{\lambda_a} \exp\left(-\frac{(\lambda_c - \lambda_a)^2}{\lambda_c}\right) \times$$

$$\left(1 - \frac{\exp[-\lambda_a(1-\lambda_a/\lambda_c)]}{\lambda_a} \sinh[\lambda_a(1-\lambda_a/\lambda_c)]\right)$$

for $r_{exo} < R_{pressure}$, $\mathcal{F} = n_{exo} U_{th}/2\sqrt{\pi}$, for $r_{exo} > R_{pressure}$ (blow-off regime); with $U_{th} = \sqrt{2 k_B T_{exo}/m}$

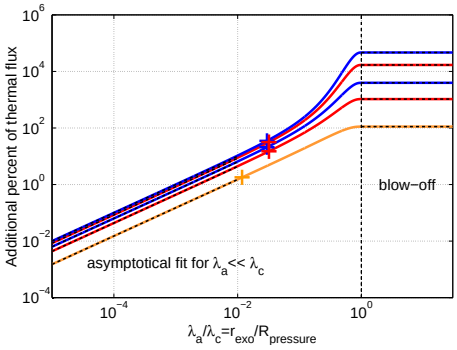

Figure 2: Relative difference between our model escape flux and the Jeans' escape flux at the subsolar point as a function of the radiation pressure at Earth (blue), Mars (red) and Titan (orange). The crosses indicate the real values at Earth (blue), Mars (red) and Titan (orange).

Finally, we study the effect of the radiation pressure on the Roche lobe position. We derive an analytical formula to determine approximatively (with a maximum error of $\sim 3\%$):

$$R_H = \frac{\beta}{9}\left(2\ \cosh\left(\frac{1}{3}\ \text{argcosh}\left(\frac{243\mu}{2\beta^3} - 1\right)\right) - 1\right)$$

for $\beta < 3\sqrt[3]{9\mu/4}$ and

$$R_H = \frac{\beta}{9}\left(2\ \cos\left(\frac{1}{3}\ \arccos\left(\frac{243\mu}{2\beta^3} - 1\right)\right) - 1\right)$$

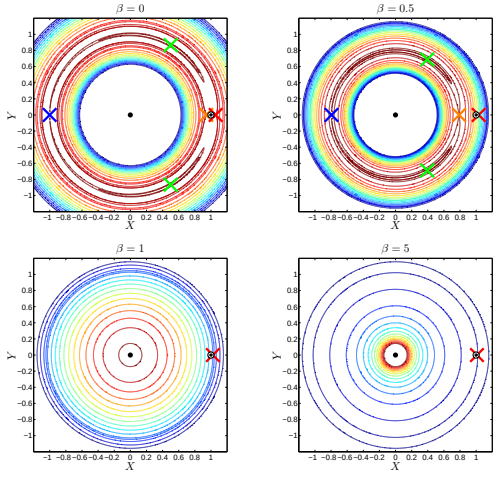

Figure 3: Levels of effective potential for Ω for $\beta = 0$ (pure CR3BP, upper panels), 0.5, 1, 5 for HD 209458b. The crosses define the Lagrange points: L_1 (orange), L_2 (red), L_3 (blue), L_4 and L_5 (green). The central point corresponds to the star position. The black point around $(1, 0)$ corresponds to the true planetary size and the surrounding white disk to the atmosphere with its supposed size.

for $\beta > 3\sqrt[3]{9\mu/4}$.

This modification could impact a lot the evolution, the escape, the stability of the surrounding atmosphere especially for Hot Jupiters. However, it could also affect strongly the primitive planetary atmospheres of the early Solar System.

3. Summary and Conclusions

We propose a semi-analytical model to estimate ballistic particles densities in planetary exospheres (in the Solar System or beyond) using Hamiltonian mechanics. We assume a collisionless exosphere. The results are in good agreement with Earth observations of day/night/dusk/dawn asymmetries. Moreover, we derive an analytical formula for the escape flux including the radiation pressure and show, for the Earth case in particular an enhancement of the escape flux by up to 30% compared with Jeans' escape formula. Finally, the radiation pressure can induce a large effect on the Three-Body, especially for planets close to their host star like HD 209458b and generally Hot Jupiters. We derive a new formula in order to determine the true size of the Hill's sphere subject to the radiation pressure.

EPSC Abstracts
Vol. 10, EPSC2015-776, 2015
European Planetary Science Congress 2015

Terrestrial and extraterrestrial landslide size statistics

M. T. Brunetti (1), Z. Xiao (2,3), G. Komatsu (4), S. Peruccacci (1) and F. Guzzetti (1)
(1) Research Institute for Geo-Hydrological Protection – Italian National Research Council, Perugia, Italy (Maria.Teresa.Brunetti@irpi.cnr.it/fax:+39-075-5014420), (2) Planetary Science Institute, China University of Geosciences, Hubei, P. R. China, (3) Centre for Earth Evolution and Dynamic, University of Oslo, Norway, (4) International Research School of Planetary Sciences, Pescara, Italy

Abstract

We present the size statistics of landslides on Earth, Mars, the Moon and Mercury. We used two existing landslide inventories for New Mexico (USA) and for Valles Marineris, Mars, and two new inventories of lunar and Mercurian landslides. Failures on the Moon and Mercury were detected and mapped along the internal walls of impact craters. The statistical distributions of the extraterrestrial landslide area were exploited to compare the results with similar distributions obtained for terrestrial landslides.

1. Introduction

Landslides play an important role in shaping the surface of the Earth and of other solid bodies, like Mars, the Moon, and Mercury. In the last decades, planetary exploration missions have released large amount of high-resolution images, which enable to detect and map morphologic structures on planetary surfaces in great detail. On Mars, large landslides have been observed mainly along the slopes of Valles Marineris, e.g. [1-2]. Numerous landslides of various scales have been observed on the Moon, e.g. [3]. On Mercury, some ejecta flows exhibit morphological similarities with mass wasting deposits on planetary surfaces. Comparison of landslide characteristics, e.g. the landslide types and sizes (area, volume, fall height, length) on different planetary bodies may help in understanding, e.g., the effect of the surface gravity on failure initiation and propagation.

2. Methodology

To compare the terrestrial and extraterrestrial landslide size statistics, we exploited a geomorphological inventory of 894 deep-seated landslides of the slide and complex types mapped in New Mexico, USA [4] and three inventories of extraterrestrial landslides. On Mars, we focused on a study area of 10^5 km^2 in Tithonium and Ius Chasmata, Valles Marineris where 189 landslides, including rock slides, complex landslides, debris flow-like failures, and rock avalanches, were previously identified and mapped [2]. Figure 1 shows an example of a rock slide on Mars.

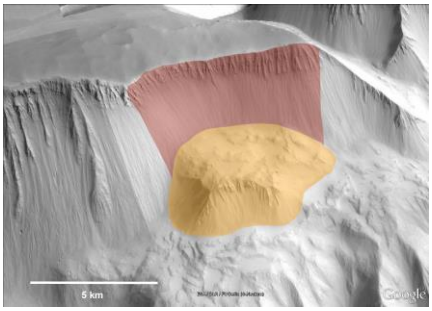

Figure 1: A rock slide in Valles Marineris, Mars. The failure scarp is in brown and the deposit is in amber.

To recognize and map landslides on the Moon and Mercury, we adopted the same visual criteria commonly used by geomorphologists to recognize terrestrial failures. On the Moon and Mercury, we focused on the large slope failures along the internal walls of impact craters. In particular, we selected and mapped landslides in simple craters, in order to deal with mass movements driven by the surface gravity and not resulting from the impact processes. For the Moon, we visually analyzed images acquired at 100 m/pixel resolution by the Wide Angle Camera onboard the Lunar Reconnaissance Orbiter Camera. For Mercury, we examined images at an average resolution of 250 m/pixel obtained by the Wide Angle Camera onboard the MESSENGER spacecraft.

3. Results

In impact craters on the Moon and Mercury, we obtained two inventories of 60 landslides mapped in 35 craters on the Moon, and 58 landslides mapped in 38 craters on Mercury. Figure 2 portrays two

examples of rock slides on the Moon (a) and on Mercury (b).

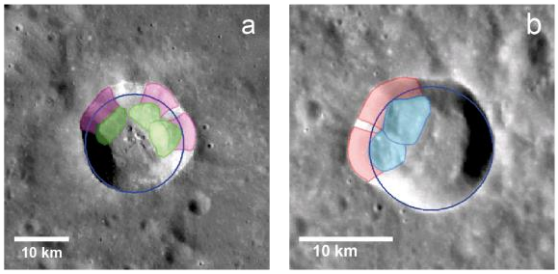

Figure 2: Rock slides on the Moon (a), and Mercury (b). Landslide scarps are in purple (a) and red (b); deposits are in green (a) and light blue (b).

Using the planimetric area, A_L, of the mapped failures we calculated the probability density distribution of the landslide area for the Moon and Mercury. Figure 3 displays the comparison between the probability density distribution, $p(A_L)$, of the landslide area, A_L, for terrestrial failures and for failures on Mars, the Moon, and Mercury.

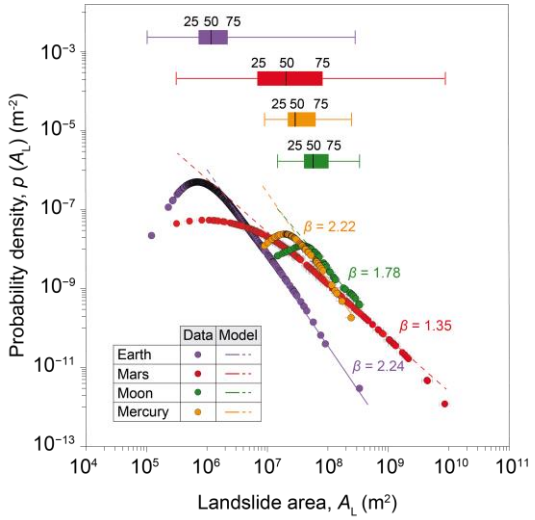

Figure 3: Probability distributions of landslide area on Earth (purple), Mars (red), the Moon (green) and Mercury (orange). Color lines show corresponding best fit models of the distribution tails. Box plots show statistics of A_L for all data sets.

Analysis of the distributions indicates that extraterrestrial landslides are larger than subaerial terrestrial landslides. On Mars, $p(A_L)$ is flatter than on other bodies. As a result, on Mars the abundance of very large landslides (A_L>10^7m^2), compared to small and medium area failures, is higher than on Earth. Lunar landslides are on average larger than failures on Mercury. We hypothesize that the stronger surface gravity of Mercury causes landslides occurring at smaller scales.

References

[1] Quantin, C., Allemand, P., and Delacourt, C.: Morphology and geometry of Valles Marineris landslides. Planet. Space Sci. 52 (11), 1011-1022, 2004.

[2] Brunetti, M.T., Guzzetti, F., Cardinali, M., Fiorucci, F., Santangelo, M., Mancinelli, P., Komatsu, G., and Borselli, L.: Analysis of a new geomorphological inventory of landslides in Valles Marineris, Mars. Earth Planet. Sci. Lett. 405, 156-168, 2014.

[3] Xiao, Z., Zeng, Z., Ding, N., and Molaro, J.:. Mass wasting features on the Moon–how active is the lunar surface? Earth Planet. Sci. Lett. 376, 1-11, 2013.

[4] Cardinali, M., Guzzetti, F., and Brabb, E.E.: Preliminary map showing landslide de-posits and related features in New Mexico. U.S. Geological Survey Open File Report 90/293, 4 sheets, scale 1:500,000, 1990.

EPSC Abstracts
Vol. 10, EPSC2015-802, 2015
European Planetary Science Congress 2015

Phobos' regolith interaction with the martian environment

F. Cipriani (1), J. Terwisscha van Scheltinga (1) , R. Modolo (2), O. Witasse (1), F. Leblanc (2)
(1) ESA/ESTEC, Noordwijk, The Netherlands, (2) LATMOS, IPSL/CNRS, Paris, France (fabrice.cipriani@esa.int / Fax: +55-555-5555555)

1. Introduction

Phobos and Deimos origins are still under debate and although formation from a debris disk following a impact seems plausible [1], other scenario such as captured objects cannot be ruled out (see [2,3] and references therein). In the case of Phobos, the latest observations in the thermal infrared range are consistent with the presence of phylosillicates, iron bearing compounds as well as mixed silicate-carbonate components and surface hydration from unclear origin [4,5]. Those observations do not allow to discriminate between different formation scenarios.

Through sputtering of the moons surfaces by solar wind, pick-up and planetary ions, surface material is continuously released in the martian environment with species somehow indicative of the moon regolith' composition.

Assuming an Iron rich composition typically matching that of D-types asteroids [6,7], production rates for Iron and Magnesium of respectively $3.04x10^{16}$ atoms.s^{-1} and $2.58x10^{16}$ atoms.s^{-1} were estimated for solar minimum conditions [8], driven mainly by solar wind ion sputtering. Pick-up ions of planetary origin have since then been reported as possibly resulting in larger sputtered fluxes under certain conditions [9].

In the present study, we simulate the sputtering of Phobos's regolith by solar wind and planetary ions for various IMF and crustal field configurations, and solar activity conditions corresponding to January to June 2015 period (F10.7 index 130). We also include ionization of the ejected neutrals by electron impact, solar photon impact, and charge exchange reactions with solar wind protons.

2. Methods and Outputs

We use a 3D Monte Carlo Test-particle numerical approach as described in [8] and references therein in order to simulate sputtering from Phobos' surface along the moon's orbit. Ejected neutrals are subject to electron impact ionization, UV solar photon impact ionization, and ionization by charge exchange with solar wind protons .

The magnetic and electric field environment at Phobos' orbit is extracted from a global multi-species parallel hybrid simulation model (LatHyS). Moreover, the model characterizes the precipitation solar wind and planetary ions (H^+ and O^+) at Phobos' surface. Simulations are performed with a spatial resolution of 80 km, however the full distribution function of the plasma in position and velocity space is provided on a uniform cartesian grid with 160km resolution. These information are used and interpolated into our test-particle simulation ~~grid~~ model. Additionally, the Martian crustal field is also modelled and might influence the planetary ions distributions at Phobos orbit.

Solar wind ions velocities and densities, IMF conditions, convection electric field, as well as planetary ions inputs (H^+ and O^+) are provided by a Hybrid model of the solar wind interaction with Mars [10], with a grid resolution of 160km which is interpolated to our test-particle simulation grid. Additionally, the martian crustal field is also modelled, as it may influence the planetary ion distributions at Phobos' orbit.

While neutral particles motion is subject to the gravity of Mars and its moons, as well as solar radiation pressure, newly created ions are picked –up by the convection electric field of the solar wind. Neutrals and ions are followed in the model until they escape the simulation domain or are lost to Mars.

We study the sensitivity of the ejected neutral clouds and of pick-up ions fluxes to the IMF and crustal field configurations, and compare our results with previous estimates. We also provide expected fluxes for major species of interest (Fe / Fe^+ and Mg / Mg^+ along Mars Express and MAVEN orbits, during close flybys with Phobos, and discuss possible analysis of data from these two spacecraft

References

[1] Robert I. Citron , Hidenori Genda, Shigeru Ida, Icarus, Volume 252, 15 May 2015, Pages 334–338

[2] Craddock, R.A., 1994. The origin of Phobos and Deimos. Lunar Planet. Sci. 25, 293 (abstract)

[3] Witasse, O. et al., 2014. Mars express investigations of Phobos and Deimos. Planet. Space Sci. 102, 18–34.

[4] Giuranna, M. et al., 2011. Compositional interpretation of PFS/MEx and TES/MGS thermal infrared spectra of Phobos. Planet. Space Sci. 59 (1), 1308–1325.

[5] T. D. Glotch1 et al abstract # 2587, 46th Lunar and Planetary Science Conference (2015)

[6] Pajola, M. et al, The Astrophysical Journal, Volume 777, Issue 2, article id. 127, 6 pp. (2013)

[7] Vernazza et al, Meteorite analogs for Phobos and Deimos: Unraveling the origin of the martian moons. In: 73rd Annual Meeting of the Meteoritical Society. Abstract #5076.

[8] Cipriani et al, A model of interaction of Phobos surface with the Martian Environment. Icarus 212 (2011) 643–648

[9] Poppe and Curry, Martian planetary heavy ion sputtering of Phobos, GeoRL, 6335-6341, 2014

EPSC Abstracts
Vol. 10, EPSC2015-832, 2015
European Planetary Science Congress 2015

What can we really say about the origin of Phobos?

P. Rosenblatt (1) and P. Lee (2)
(1) Royal Observatory of Belgium, Belgium, (2) NASA-AMES, USA, (rosenb@oma.be / Fax: +32 373 67 30)

Abstract

There has been a renewed interest in the scientific investigation of Phobos and Deimos in recent years, in particular with the new observations of the former by ESA's Mars Express mission [1]. The origin of Phobos remains an especially vexing mystery [2]. This has reinforced interest worldwide, at ESA, ROSCOSMOS, NASA, and JAXA, to include Phobos as a potential target for future missions. Here, we review recent observations of the surface and interior of Phobos, as well as modeling efforts, to see where we stand on the formation of both Phobos and Deimos.

1. Introduction

The origin of the two small Martian moons is one of the most mysterious in our solar system in spite of the numerous spacecraft mission sent to the Martian system. They could be either primitive objects captured by Mars or formed in Mars' orbit. The numerous data collected by at least 6 Martian spacecraft have not allowed deciphering between those two distinct scenarios of origin. Although variant of these scenarios have been proposed, all of them are flawed and data to fix that issue have not all been acquired yet. Phobos and Deimos are two small bodies easy to access and appear now as privileged targets for space agencies aiming to study the small celestial bodies too. The study of the Martian moons concern also the formation and the early dynamics of the solar system, and even the formation of the moons in the exo-planetary systems.

2. The capture scenario

The science community has accepted this scenario since the NASA Viking missions. Nevertheless, this scenario suffers weakness and disagreement between the observations and modeling. The main observational argument supporting the capture scenario is the reflectance spectra of the surface in the visible and near infrared (Vis-NiR) domain. These spectra look like those of primitive asteroid [3 and references therein]. However, no prominent absorption features, which are the diagnostic of the composition, have been identified in these spectra so far [4]. The Phobos and Deimos spectra are indeed flat and reddened as for highly space-weathered surfaces. Recently, emissivity spectra in the thermal infrared (IR) domain have been performed. Clear signatures are visible unlike Vis/NiR spectra. But these signatures have been interpreted either as silicate material [5] or as carbonaceous primitive material [6]. On the other hand, the capture scenario has serious issues to account for the capture in Mars' orbit and for the current near-equatorial and near-circular orbits of the moons. The first step of capture would be feasible, although assuming a "kick-off" through a collisional event in or close to Mars' orbit between two former bodies [7]. However, the post-capture orbital changes by tidal dissipation of orbital energy inside Mars and Phobos would need too high dissipation rate in Phobos (closer to icy material than to rocky material) in order to reach the current orbit (e.g. [8]). The required orbital changes for Deimos even require orbital evolution over more than the age of the solar system. Although several alternatives have been proposed to help the orbital changes after capture, not all have been thoroughly studied and none of them have been shown to work properly [2].

3. The *in-situ* formation

Several authors have proposed alternative scenarios of formation of both moons in Mars' orbit. One of them has recently retained the attention of scientific community. This scenario largely relies on the formation of the Earth's moon, i.e. re-accretion of debris blasted into Mars' orbit after a giant collision [9]. The formation of the circum-Mars disk after a giant collision has been modeled, and has shown that most of the material of the disk is concentrated close to Mars below the Roche limit (at about 2.5 Mars Radii) [10]. Nevertheless, the moonlets formed from such a disk could not reach the synchronous limit (at 6 Mars radius) before the disk be emptied primarily from its inner edge and then the moonlet orbit recede back to Mars [11]. Such an accretion disk and associated moonlet system is thus expected to last not more than about 200 millions of years that is in

strong contradiction with the surface age of Phobos estimated as old as 4.0 +/- 0.4 billions of years [12] and also with the current position of Deimos beyond the synchronous distance to Mars.

2. The interior of Phobos

The Mars Express (MEX) mission has allowed probing the interior of Phobos with unprecedented accuracy. The mass and the volume have been dramatically improved and the density very accurately determined. The low density of Phobos (less than 1.9 $g.cm^3$) strongly argues in favor of a compositionally and even structurally heterogeneous interior [2]. The libration amplitude has also been measured by MEX. Its value is close to the one expected for homogeneous Phobos (either monolithic Phobos interior or well-mixed compositionally heterogeneous Phobos interior) [13]. Nevertheless, the error bar is still as large as 14% and recovers the expected values for heterogeneous mass distribution obtained with interior models of Phobos containing, rocks, ice and voids [14]. The gravity field coefficients of Phobos, related to its internal mass distribution (along with the libration amplitude) have also been measured by MEX, but with an error bar close to 100% [15], thus precluding to identify the nature of possible heterogeneous mass distribution inside Phobos.

4. How to say more?

The most obvious lacking observation that will decisively help to decipher along scenarios of the origin of Phobos is its composition: What Phobos is made of? A return sample mission is certainly the best way to remove any ambiguity from remote sensing data. Nevertheless, one single sampling area would not necessarily represent both surface variability as suggested by the so-called red and blue spectral units [4] and bulk interior. The knowledge of interior homogeneity is useful test of our ability to extrapolate surface composition derived from returned sampling to the bulk body. Probing the interior of the bulk Phobos is therefore mandatory as well as a precise and complete characterization of the sampling area using former, but more precise, observations as well as new ones not performed at Phobos so far. For instance, determining whether Phobos interior contains water ice is a key element as to decipher its origin. Such ambitious new data could be acquired on orbit and on landing phases in one single mission or on two folds missions, depending on allowed cost and programmatic of space agencies.

5. Summary and Conclusions

Several missions to Phobos have been recently proposed to ESA and NASA exploration programs (e.g. [16]) and others are currently studied at ESA and Roscosmos. Beyond the Martian system origin, deciphering the origin of Phobos and Deimos will put additional constraints to the planetary formation and the early stage of solar system history. Indeed, if Phobos contains significant amount of water-ice, it might be a relieve of bodies spread from the outer to the inner solar system by dynamical instabilities in the first hundreds of millions of years of solar system history [17]. A better understanding of the formation of both Martian moons would bring clearer views in the processing of formation of moons around terrestrial planets that will have to be assessed with future observations of moons around extra-solar planets (i.e. exo-moons). Eventually, Phobos and Deimos offers accessible targets for sample return of the Martian system before the most challenging sample return of Mars surface.

Acknowledgements

PR is financially supported by the Belgian PRODEX program managed by the European Space Agency in collaboration with the Belgian Federal Science Policy Office.

References

[1] Witasse et al., Planet. Space Sci., Vol. 102, pp. 18-34, 2014; [2] Rosenblatt P., Astron. Astrophys. Rev., Vol. 19, pp. 1-26, 2011; [3] Pajola et al., Astrophys. J., Vol. 777, 6 pages, 2013; [4] Pieters et al., Planet. Space Sci., Vol. 102, pp. 144-151, 2014; [5] Giuranna M. et al., Planet Space Sci., Vol. 59, pp. 1308-1325, 2011; [6] Glotch et al., 46th LPSC, Houston, TX, USA, 2015; [7] Pajola et al., Mon. Not. R. Astron. Soc., Vol. 427, pp. 3230-3243, 2012; [8] Rosenblatt P. and Pinier B., 5MS3 13-17 October, Moscow, Russia, 2014; [9] Craddock R.A., Icarus, Vol. 211, pp. 1150-1161, 2011; [10] Citron R. et al., Icarus, Vol. 252, pp. 334-338, 2015; [11] Rosenblatt P. and Charnoz S., Icarus, Vol. 221, pp. 806-815, 2012; [12] Schmedemann N. et al., Planet. Space Sci., Vol. 102, pp. 152-163; [13] Oberst et al., Planet. Space Sci., Vol. 102, pp. 45-50, 2014; [14] Rosenblatt P. et al., EPSC, 24-28 September, Madrid, Spain, 2012; [15] Paetzold M. et al., Icarus, Vol. 229, pp. 92-98, 2014; [16] Lee, P. et al., 46th LPSC, Houston, TX, USA, 2015; [17] Tsiganis K. et al., Nature, vol. 435, pp. 459-461; 2005.

EPSC Abstracts
Vol. 10, EPSC2015-839, 2015
European Planetary Science Congress 2015

Planning the HRIC (High Resolution Imaging Channel) observations of Mercury surface

M. Zusi (1, 2), G. Di Achille (3), V. Galluzzi (4), E. Mazzotta Epifani (5), V. Della Corte (2), P. Palumbo (4), E. Flamini (7)
(1) INAF-OAC, Naples, Italy, (2) INAF-IAPS, Rome, Italy, (3) INAF-OATe, Teramo, Italy, (4) Università Parthenope, Naples, Italy, (5), INAF-OAR, Rome, Italy, (6) ASI, Rome, Italy (zusi@na.astro.it)

Abstract

The High Resolution Imaging Channel (HRIC) of SIMBIO-SYS [1] onboard the BepiColombo mission to Mercury, is the visible imaging camera devoted to the detailed characterization of the Hermean surface. The potential huge amount of data that HRIC can produce must cope with the allocated (and shared) mission resources in terms of power, data volume, and pointing maneuvers. For this reason, well before the mission launch, it is extremely important the definition of an operative plan compatible with both the available resources and the scientific objectives accomplishment.

1. Introduction

With its 2.5"/pxl angular resolution and a 4Mpx Hybrid Si-PIN CMOS sensor [2], HRIC acquires 150 square kilometers footprints images (at 480 km of altitude) which correspond to about 0.0002% of Mercury surface that rises up to about 10% when considering the mean 8 Mbit for compressed full-frame acquisition [3] and the allocated data volume. The latter figures immediately show that HRIC operation plan must be carefully defined to guarantee the satisfaction of scientific objectives in compliance with the available resources.

2 Observation planning strategy

The core strategy for the definition of a HRIC observation plan is to build a set of realistic, scientifically interesting and resource-feasible operative scenarios through the following steps:

- build a database of high priority scientific targets based mostly on MESSENGER data and recent results
- simulate target observations using the ESA MAPPS (Mapping and Planning Payload Science) tool to retrieve the synthetic footprints and the report in terms of resource allocation
- evaluate occurrence and quality of planned observations by importing all the MAPPS footprints and geometrical data (e.g., illumination angle) and radiometric conditions into GIS (Geographic Information System) environment
- prioritize targets as a trade-off between their scientific relevance, possible observational windows, quality of acquisition parameters, and the resource demand availability

Finally, since the prioritizing phase could evidence the infeasibility of some observations, the initial observables database must be updateable / extendible to integrate additional interesting areas.

2.1 Definition of interesting areas

The definition of the observables database represents a long and complex task since it requires to:

- collect all latest images (e.g., MESSENGER-MDIS data)
- build the GIS database
- identify all Mercury's geological units and interesting features such as hollows, volcanic vents, tectonic structures, etc.

The geological map of the Victoria quadrangle [4] represents a solid and complete reference for building a preliminary database of observables.

2.2 Observation simulations

Pending the completion of a global Mercury geological map, a simulation of HRIC operations has been done considering the presently known Mercury geological units (i.e., USGS database).

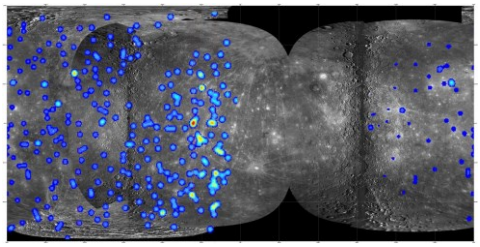

Figure 1: Mercury's topographic map with USGS surface features (blue spots).

Potential targets have been imported in GIS environment and compared with the HRIC footprints computed with the ESA MAPPS tool to compute the real HRIC operations in terms of resources and computation demands (i.e., data volume, power, special pointing requests).

2.3 Observations quality evaluation

Resulting footprints are then filtered considering geometrical (e.g., illumination angle, umbra) and radiometric (e.g., SNR [5], image contrast) conditions (Figure 2). Once completed the MAPPS simulations for all defined observational targets, the on-orbit data production profile has been computed (Figure 3).

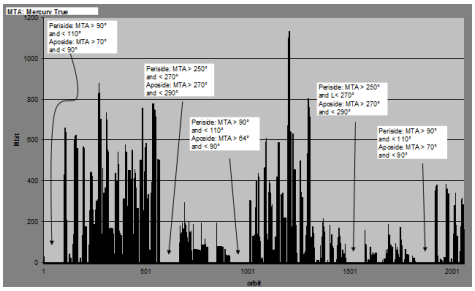

Figure 3: HRIC data volume per orbit.

2.4 Target prioritization and database update

On the completion of the scientific and performance evaluation of the observables plan, the ESA SGS team is involved in comparing the observable plan of all BepiColombo instruments to find out possible conflicts and/or opportunities and to allow an optimal usage of mission resources (Figure 4).

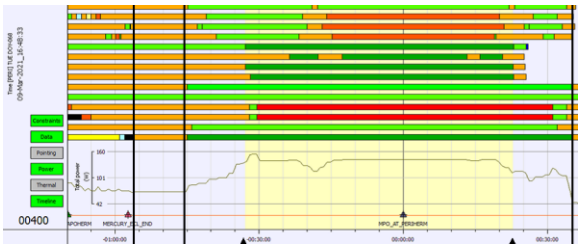

Figure 4: Instrument resource demand comparison.

Operation conflicts (e.g., not enough power, incompatible pointing maneuvers, operation cross-interferences) are then scientifically discussed between the involved teams eventually considering revisions of the observational targets database.

Acknowledgements

We gratefully acknowledge funding from the Italian Space Agency (ASI) under contract I/022/10/0. Special thanks to my wife Katia and my beautiful son Emanuele for supporting my work every day.

References

[1] Flamini, E., et al.: SIMBIO-SYS: The spectrometer and imagers integrated observatory system for the BepiColombo planetary orbiter, Planetary and Space Science, Vol. 58, p. 125, 2010.

[2] Marra, G., et al.: The Optical Design of the High Resolution Imaging Channel for the SIMBIO-SYS experiment on the BepiColombo Mission to Mercury, Memorie della Società Astronomica Italiana Supplement, v.12, p.77, 2008.

[3] Langevin, Y., et al.: Image and spectral image compression for four experiments on the ROSETTA and Mars Express missions of ESA, Proc. SPIE Vol. 4115, p. 364, 2000.

[4] Galluzzi, V., et al.: Geologic map and structural analysis of the Victoria quadrangle, Mercury, Geophysical Research Abstracts Vol. 17, EGU2015-14857.

[5] Zusi, M., et al.: Radiometric Model and Operation-Define-Tool for HRIC SIMBIO-SYS on the BepiColombo mission to Mercury, Memorie della Società Astronomica Italiana Supplement, v.12, p.72, 2008.

EPSC Abstracts
Vol. 10, EPSC2015-888, 2015
European Planetary Science Congress 2015

Phobos interior structure from its gravity field

S. Le Maistre (1), P. Rosenblatt (2), A. Rivoldini (2)
(1) Jet Propulsion Laboratory, California Institute of Technology, Pasadena, CA 91109, USA,
(2) Royal Observatory of Belgium, av. Circulaire 3, Brussels 1180, Belgium.
(sebastien.le.maistre@jpl.nasa.gov / Tel: +1-818-354-4381)

Abstract

Phobos origin remains mysterious. It could be a captured asteroid, or an in-situ object co-accreted with Mars or formed by accretion from a disk of impact ejecta.
Although it is not straightforward to relate its interior properties to its origin, it is easy to agree that the interior properties of any body has to be accounted for to explain its life's history. What event could explain such an internal structure? Where should this object formed to present such interior characteristics and composition?
We perform here numerical simulations to assess the ability of a gravity experiment to constrain the interior structure of the martian moon Phobos, which could in turn allow distinguishing among the competing scenarios for the moon's origin.

1. Introduction

As surprising as it may seem given the numerous missions already sent to the martian system, the question of the origin of Phobos is still an open issue (e.g. Rosenblatt et al. this meeting). Where does Phobos come from? To unveil this mystery, the science community is more and more pushing the space agencies to dedicate a mission to the martian moons. The mission concepts recently proposed by different groups across the world (e.g. Pandora [1], PADME [2], MERLIN [3], PhoDEx [4]) all agree with the fact that the origin of Phobos can be revealed by combining different kinds of observation (e.g. imagerie, spectroscopy, radio, sample return, etc.).
Le Maistre et al. (2013) [5] used radio-tracking data from a lander mission to measure the libration amplitude and infer the moment of inertia of Phobos. Here we use similar data but obtained from a spacecraft in orbit around the moon long enough to accurately estimate his first degree and order gravity coefficients. Based on such data, and considering a couple of mission scenarios, predictions on the gravity harmonic coefficient uncertainties are first provided. Then, we construct models of mass repartition for a heterogeneous Phobos' interior composed of rocks, volatile (water ice) and porosity to predict the range of possible values for the gravity coefficients. We finally discuss the ability of an orbiting mission to provide constraints on the interior structure of Phobos based on radio-science data.

2. Gravity field determination

The radio-science data, sensitive to the mass distribution inside the body, are commonly used to determine the gravity field of a celestial body through precise orbit determination technics. We here show that, given the mission scenario recently proposed by different groups (see examples listed above), the degree 2 gravity field of Phobos could be estimated very precisely with a precision better than 0.1%. We also show that a determination of the gravity field up to degree 10 could be reached for a long enough mission, orbiting close enough to the surface of the moon.

3. Signature of the interior in the gravity field

In order to study the effect of the internal structure on the gravity field coefficients we build a 3 dimensional model of Phobos interior by discretizing the volume in a set of cubes of equal size [6]. Based on a random process, we first show the dependency of the low degree gravity field to the proportion and density of the assumed rocky material composing Phobos (see Fig. 1 as an example for C_{20}). Because of its small size and mass, Phobos could have very puzzling interior structure. We focus in a second part of the study on a few typical interior we found in the literature in order to see if gravity data will enable to discriminate between them.

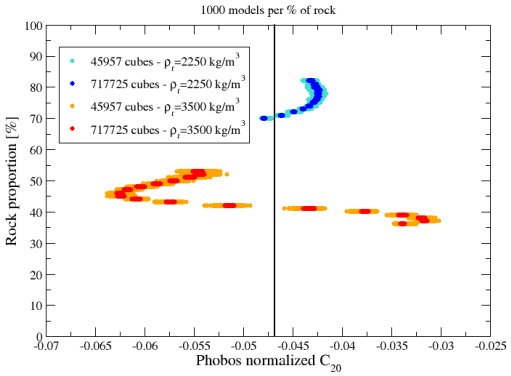

Figure 1: $C_{2,0}$ possible value as a function of the rock density, proportions of rock and cubes number. The black vertical line is the expected value for an homogeneous Phobos.

4. Conclusions

Here we study Phobos' gravity field for different plausible interior structure models. We show the signature of structural and compositional heterogeneities in the gravity field harmonics coefficients and we finally discuss the ability of a gravity experiment to discriminate between the different interior properties of Phobos proposed in the literature.

Acknowledgements

The research carried out at the Jet Propulsion Laboratory was supported by an appointment to the NASA Post-doctoral Program at the Jet Propulsion Laboratory, administered by Oak Ridge Associated Universities through a contract with NASA. The other part of this study is financially supported by the Belgian PRODEX program managed by the European Space Agency in collaboration with the Belgian Federal Science Policy Office.

References

[1] C. A. Raymond, T. H. Prettyman, and S. Diniega. PANDORA -Unlocking the Mysteries of the Moons of Mars. In *Lunar and Planetary Science Conference*, volume 46, page 2792, March 2015.

[2] P. Lee, M. Benna, D. Britt, A. Colaprete, W. Davis, G. Delory, R. Elphic, E. Fulsang, A. Genova, D. Glavin, W. Grundy, W. Harris, B. Hermalyn, B. Hine, M. Horanyi, D. Hamilton, R. Johnson, T. Jones, S. Kempf, B. Lewis, L. Lim, P. Mahaffy, J. Marshall, P. Michel, D. Mittlefehldt, S. Montez, Y. Nguyen, B. Owens, M. Pajola, R. Park, C. Phillips, L. Plice, A. Poppe, J. E. Riedel, A. Rivoldini, P. Rosenblatt, M. Schaible, M. Showalter, H. Smith, Z. Sternovsky, P. Thomas, H. Yano, and M. Zolensky. PADME (Phobos and Deimos and Mars Environment): A Proposed NASA Discovery Mission to Investigate the Two Moons of Mars. In *Lunar and Planetary Science Conference*, volume 46, page 2856, March 2015.

[3] S. L. Murchie, N. L. Chabot, J. C. Castillo-Rogez, R. E. Arvidson, D. L. Buczkowski, D. A. Eng, A. B. Chmielewski, J. N. Maki, A. Trebi-Ollenu, B. L. Ehlmann, P. N. Peplowski, H. E. Spence, M. Horanyi, G. Klingelhoefer, J. A. Christian, and C. M. Ernst. The Mars-Moons Exploration, Reconnaissance and Landed Investigation. In *Lunar and Planetary Science Conference*, volume 46, page 2047, March 2015.

[4] J. Oberst, K. Wickhusen, K. Willner, and the PhoDEx Team. PhoDEx - a mission to explore the interiors of Phobos and Deimos. In *EGU General Assembly 2015, held 12-17 April, 2015 in Vienna, Austria*, volume 17, page 15235, April 2015.

[5] S. Le Maistre, P. Rosenblatt, N. Rambaux, J. C. Castillo-Rogez, V. Dehant, and J-C. Marty. Phobos interior from librations determination using Doppler and star tracker measurements. *Planetary and Space Science*, 85:106–122, September 2013.

[6] A. Rivoldini, P. Rosenblatt, and S. Le Maistre. The interior structure of Phobos. *In preparation*, 2015.